Far-zone behaviors of scattering-induced statistical properties of partially polarized spatially and spectrally partially coherent electromagnetic pulsed beam*

Yan Li(李艳), Ming Gao(高明)†, Hong Lv(吕宏), Li-Guo Wang(王利国), and Shen-He Ren(任神河)

School of Optoelectronic Engineering, Xi'an Technological University, Xi'an 710021, *China*

(Received 8 March 2020; revised manuscript received 22 April 2020; accepted manuscript online 18 June 2020)

In this study, we explore the far-zero behaviors of a scattered partially polarized spatially and spectrally partially coherent electromagnetic pulsed beam irradiating on a deterministic medium. The analytical formula for the cross-spectral density matrix elements of this beam in the spherical coordinate system is derived. Within the framework of the first-order Born approximation, the effects of the scattering angle θ, the source parameters (*i.e.*, the pulse duration T_0 and the temporal coherence length T_{cxx}), and the scatterer parameter (*i.e.*, the effective width of the medium σ_R) on the spectral density, the spectral shift, the spectral degree of polarization, and the degree of spectral coherence of the scattered source in the far-zero field are studied numerically and comparatively. Our work improves the scattering theory of stochastic electromagnetic beams and it may be useful for the applications involving the interaction between incident light waves and scattering media.

Keywords: scattering, partially polarized spatially and spectrally partially coherent electromagnetic pulsed beam, statistical properties, deterministic medium

PACS: 42.25.Fx, 42.25.Ja, 42.25.Kb **DOI:** 10.1088/1674-1056/ab9de7

1. Introduction

The statistical characteristics of a scattering medium are directly associated with the properties of the incident source and the scatterer. Thus, the cross-spectral density (CSD) of the far-zero scattered field is measured in order to acquire the specific information about the scatterer.[1–5] The scattering of light wave is of great interest due to its wide application in optical communication, medical imaging, and remote sensing.[6] In the past several decades, the findings about scattering media have focused on various types of scattering media, such as a deterministic medium,[1–3,7,8] a collection of particles,[4] and a random medium including a quasi-homogeneous media,[9] a Gaussian Schell-model random medium,[10,11] a semisoft boundary medium,[12] a non-Gaussian-correlated medium,[13] and a quasi-homogeneous anisotropic medium.[14] Additionally, the incident sources have also been extended from monochromatic or polychromatic, scalar or vector plane waves to more common beams, such as partially coherent beams,[15,16] stochastic electromagnetic beams,[7,17,18] plane-wave pulses,[3,19] and vortex beams.[8] For these incident sources, considerable work has been done in illustrating the scattering processes based on the theory of the first-order Born approximation.[7–19] However, most of the existing studies were restricted to the situation in which the incident source was statistically stationary, at least in the wide sense.[4–17] To date, only a few studies have focused on a non-stationary source.[2,3,18,19]

A typical non-stationary stochastic source called spatially and spectrally partially coherent pulses was introduced by Lajunen *et al.*[20] By extending the notion of the CSD matrix from stochastic electromagnetic stationary beams to stochastic electromagnetic pulsed beams, we explored the propagation properties of a partially polarized spatially and spectrally partially coherent electromagnetic Gaussian Schell-model pulsed (EGSMP) beam in a turbulent atmosphere.[21–23] To the best of our knowledge, an investigation of the statistics of a partially polarized spatially and spectrally partially coherent electromagnetic pulse irradiating on a deterministic scattering medium has not been presented thus far. For this reason, based on the theory of the first-order Born approximation, we explore the case of a partially polarized spatially and spectrally partially coherent EGSMP beam interacting with a deterministic scattering medium. The statistical properties such as the spectral intensity, the spectral shift, the spectral degree of polarization, and the degree of spectral coherence of this scattered beam in the far-zero field are discussed in detail in this paper. Some interesting results are obtained.

2. Theoretical formulation

We begin our discussion by considering a planar, stochastic electromagnetic, statistically non-stationary source that is incident on a deterministic scattering medium. In the space–time domain, the statistics of this source can be defined by a 2×2 mutual coherence function (MCF) matrix. This matrix

*Project supported by the National Natural Science Foundation of China (Grant No. 11504286), the Natural Science Basic Research Program of Shaanxi Province, China (Grant No. 2019JM-470), the Fund from the International Technology Collaborative Center for Advanced Optical Manufacturing and Optoelectronic Measurement, and the Science Fund from the Shaanxi Provincial Key Laboratory of Photoelectric Measurement and Instrument Technology.

†Corresponding author. E-mail: minggao1964@163.com

can be expressed in the following form

$$\boldsymbol{\Gamma}^{(0)}(\boldsymbol{\rho}_1,\boldsymbol{\rho}_2,t_1,t_2) = \begin{bmatrix} \Gamma_{xx}^{(0)}(\boldsymbol{\rho}_1,\boldsymbol{\rho}_2,t_1,t_2) & \Gamma_{xy}^{(0)}(\boldsymbol{\rho}_1,\boldsymbol{\rho}_2,t_1,t_2) \\ \Gamma_{yx}^{(0)}(\boldsymbol{\rho}_1,\boldsymbol{\rho}_2,t_1,t_2) & \Gamma_{yy}^{(0)}(\boldsymbol{\rho}_1,\boldsymbol{\rho}_2,t_1,t_2) \end{bmatrix}, \quad (1)$$

where

$$\Gamma_{\alpha\beta}^{(0)}(\boldsymbol{\rho}_1,\boldsymbol{\rho}_2,t_1,t_2) = [\langle E_\alpha^*(\boldsymbol{\rho}_1,t_1)\, E_\beta(\boldsymbol{\rho}_2,t_2)\rangle]$$

for $\alpha,\beta = x,y$, with the asterisk being the complex conjugate, and the angular bracket being the ensemble average. For a partially polarized spatially and spectrally partially coherent EGSMP beam,

$$\begin{aligned}&\Gamma_{\alpha\beta}^{(0)}(\boldsymbol{\rho}_1,\boldsymbol{\rho}_2,t_1,t_2)\\ &= A_\alpha A_\beta B_{\alpha\beta}\exp\left[-\frac{\rho_1^2+\rho_2^2}{4w_0^2}-\frac{(\boldsymbol{\rho}_1-\boldsymbol{\rho}_2)^2}{2\delta_{\alpha\beta}^2}\right]\\ &\times\exp\left[-\frac{t_1^2+t_2^2}{2T_0^2}-\frac{(t_1-t_2)^2}{2T_{c\alpha\beta}^2}\right]\exp\left[\mathrm{i}\omega_0(t_1-t_2)\right],\\ &(\alpha,\beta=x,y), \end{aligned} \quad (2)$$

that is, $\Gamma_{\alpha\beta}^{(0)}(\boldsymbol{\rho}_1,\boldsymbol{\rho}_2,t_1,t_2)$ is composed of separable space-dependent part and time-dependent part.[20] A_α and A_β are the average amplitudes of the α and β electric field components, respectively, $B_{\alpha\beta}$ represents the correlation coefficient between α and β electric field components. These components have the following characteristics:[21,23] $B_{\alpha\beta}\equiv 1$ for $\alpha=\beta$, $|B_{\alpha\beta}|\le 1$ for $\alpha\neq\beta$, and $B_{xy}=B_{yx}^*=|B_{xy}|\exp(\mathrm{i}\psi)$, ψ is the phase difference, $\psi\neq k\pi$ ($k=1,2,3,\ldots$). w_0 and $\delta_{\alpha\beta}$ are the beam width and the spatial coherence width, respectively. ω_0 is the central frequency of the pulse, T_0 is the pulse duration, and $T_{c\alpha\beta}$ is the temporal coherence width of the pulse.

According to the extended Wiener–Khintchine theorem,[23] we have

$$\begin{aligned}&W_{\alpha\beta}^{(0)}(\boldsymbol{\rho}_1,\boldsymbol{\rho}_2,\omega_1,\omega_2)\\ &= \frac{1}{(2\pi)^2}\iint\Gamma_{\alpha\beta}^{(0)}(\boldsymbol{\rho}_1,\boldsymbol{\rho}_2,t_1,t_2,)\\ &\times\exp[-\mathrm{i}(\omega_1 t_1-\omega_2 t_2)]\,\mathrm{d}t_1\,\mathrm{d}t_2, \end{aligned} \quad (3)$$

that is, the MCF and the CSD form a Fourier-transform pair. When equation (2) is substituted into Eq. (3), the following formula is obtained

$$\boldsymbol{W}^{(0)}(\boldsymbol{\rho}_1,\boldsymbol{\rho}_2,\omega_1,\omega_2) = \begin{bmatrix} W_{xx}^{(0)}(\boldsymbol{\rho}_1,\boldsymbol{\rho}_2,\omega_1,\omega_2) & W_{xy}^{(0)}(\boldsymbol{\rho}_1,\boldsymbol{\rho}_2,\omega_1,\omega_2) \\ W_{yx}^{(0)}(\boldsymbol{\rho}_1,\boldsymbol{\rho}_2,\omega_1,\omega_2) & W_{yy}^{(0)}(\boldsymbol{\rho}_1,\boldsymbol{\rho}_2,\omega_1,\omega_2) \end{bmatrix}, \quad (4)$$

with

$$\begin{aligned}&W_{\alpha\beta}^{(0)}(\boldsymbol{\rho}_1,\boldsymbol{\rho}_2,\omega_1,\omega_2)\\ &= \frac{A_\alpha A_\beta B_{\alpha\beta}T_0}{2\pi\Omega_{0\alpha\beta}}\exp\left[-\frac{\rho_1^2+\rho_2^2}{4w_0^2}-\frac{(\boldsymbol{\rho}_1-\boldsymbol{\rho}_2)^2}{2\delta_{\alpha\beta}^2}\right]\\ &\times\exp[-T_{\alpha\beta}(\omega_1,\omega_2)], \end{aligned} \quad (5)$$

where

$$T_{\alpha\beta}(\omega_1,\omega_2) = \frac{(\omega_1-\omega_0)^2+(\omega_2-\omega_0)^2}{2\Omega_{0\alpha\beta}^2}+\frac{(\omega_1-\omega_2)^2}{2\Omega_{c\alpha\beta}^2}, \quad (6)$$

with

$$\Omega_{0\alpha\beta} = \sqrt{1/T_0^2+2/T_{c\alpha\beta}^2},$$
$$\Omega_{c\alpha\beta} = \sqrt{T_0^2+T_{c\alpha\beta}^2}/T_0^2$$

describing the spectral width and the spectral coherent width of the pulse, respectively.[22]

Based on the CSD matrix of an electromagnetic pulsed beam, there are three important fundamental statistical properties of the incident field that could be defined as the average spectral intensity,[23]

$$\begin{aligned}S_0(\boldsymbol{\rho},\omega) &= \mathrm{Tr}\left[\boldsymbol{W}^{(0)}(\boldsymbol{\rho},\boldsymbol{\rho},\omega,\omega)\right]\\ &= \frac{A_x^2B_{xx}T_0}{2\pi\Omega_{0xx}}\exp\left[-\frac{\rho^2}{2w_0^2}-\frac{(\omega-\omega_0)^2}{\Omega_{0xx}^2}\right]\\ &+\frac{A_y^2B_{yy}T_0}{2\pi\Omega_{0yy}}\exp\left[-\frac{\rho^2}{2w_0^2}-\frac{(\omega-\omega_0)^2}{\Omega_{0yy}^2}\right], \end{aligned} \quad (7)$$

the spectral degree of polarization (DOP),[22]

$$P_0(\boldsymbol{\rho},\omega) = \sqrt{1-\frac{4\mathrm{Det}\boldsymbol{W}^{(0)}(\boldsymbol{\rho},\boldsymbol{\rho},\omega,\omega)}{\mathrm{Tr}^2\,\boldsymbol{W}^{(0)}(\boldsymbol{\rho},\boldsymbol{\rho},\omega,\omega)}}. \quad (8)$$

(i) For B_{xy}= 0,

$$P_0(\boldsymbol{\rho},\omega) = \left|\frac{\frac{A_x^2B_{xx}}{\Omega_{0xx}}\exp\left[-\frac{(\omega-\omega_0)^2}{\Omega_{0xx}^2}\right]-\frac{A_y^2B_{yy}}{\Omega_{0yy}}\exp\left[-\frac{(\omega-\omega_0)^2}{\Omega_{0yy}^2}\right]}{\frac{A_x^2B_{xx}}{\Omega_{0xx}}\exp\left[-\frac{(\omega-\omega_0)^2}{\Omega_{0xx}^2}\right]+\frac{A_y^2B_{yy}}{\Omega_{0yy}}\exp\left[-\frac{(\omega-\omega_0)^2}{\Omega_{0yy}^2}\right]}\right|; \quad (9)$$

(ii) For $B_{xy}\neq 0$,

$$P_0(\boldsymbol{\rho},\omega) = \frac{\sqrt{p_2^2(\omega)+4p_3^2(\omega)}}{p_1(\omega)}, \quad (10)$$

where

$$\begin{aligned}p_1(\omega) &= \frac{A_x^2B_{xx}}{\Omega_{0xx}}\exp\left[-\frac{(\omega-\omega_0)^2}{\Omega_{0xx}^2}\right]\\ &+\frac{A_y^2B_{yy}}{\Omega_{0yy}}\exp\left[-\frac{(\omega-\omega_0)^2}{\Omega_{0yy}^2}\right], \end{aligned}$$

$$p_2(\omega) = \frac{A_x^2 B_{xx}}{\Omega_{0xx}} \exp\left[-\frac{(\omega-\omega_0)^2}{\Omega_{0xx}^2}\right] - \frac{A_y^2 B_{yy}}{\Omega_{0yy}} \exp\left[-\frac{(\omega-\omega_0)^2}{\Omega_{0yy}^2}\right],$$
$$p_3^2(\omega) = \frac{A_x^2 A_y^2 |B_{xy}|^2}{\Omega_{0xy}^2} \exp\left[-\frac{2(\omega-\omega_0)^2}{\Omega_{0xy}^2}\right], \quad (11)$$

and the spectral degree of coherence (DOC)[24]

$$\mu(\boldsymbol{\rho},\boldsymbol{\rho},\omega_1,\omega_2) = \frac{\sqrt{\mathrm{Tr}\left[\boldsymbol{W}^{(0)}(\boldsymbol{\rho},\boldsymbol{\rho},\omega_1,\omega_2)\boldsymbol{W}^{(0)*}(\boldsymbol{\rho},\boldsymbol{\rho},\omega_1,\omega_2)\right]}}{\sqrt{\boldsymbol{S}(\boldsymbol{\rho},\omega_1)\boldsymbol{S}(\boldsymbol{\rho},\omega_2)}}. \quad (12)$$

In Eqs. (7)–(12), Det and Tr are the determinant and the trace of the CSD matrix, respectively. It can be found in Eqs. (7)–(12) that A_x, A_y, $B_{\alpha\beta}$, T_0, and $T_{c\alpha\beta}$ are the key parameters that determine the statistical properties of the incident field.

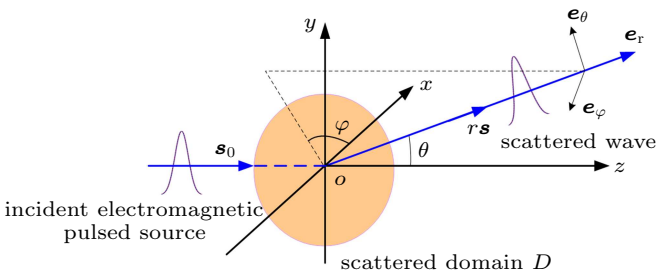

Fig. 1. Illustration of symbols relating to incident partially polarized spatially and spectrally partially coherent electromagnetic pulsed source irradiating on deterministic scattering medium in spherical coordinate system.

Figure 1 shows that the partially polarized spatially and spectrally partially coherent EGSMP source is incident along the direction of a real unit vector $\boldsymbol{s}_0(p, q, \sqrt{1-p^2-q^2})$ on a linear, isotropic, statistically stationary non-magnetic medium occupying a finite domain D in free space. The physical properties of the incident field at any two vectors $\boldsymbol{r}_1$ and $\boldsymbol{r}_2$ can be described by the CSD matrix. This matrix is expressed as[2]

$$\boldsymbol{W}^{(i)}(\boldsymbol{r}_1,\boldsymbol{r}_2,\boldsymbol{s}_{01},\boldsymbol{s}_{02},\omega_1,\omega_2) = \begin{bmatrix} W_{xx}(\boldsymbol{r}_1,\boldsymbol{r}_2,\boldsymbol{s}_{01},\boldsymbol{s}_{02},\omega_1,\omega_2) & W_{xy}(\boldsymbol{r}_1,\boldsymbol{r}_2,\boldsymbol{s}_{01},\boldsymbol{s}_{02},\omega_1,\omega_2) \\ W_{yx}(\boldsymbol{r}_1,\boldsymbol{r}_2,\boldsymbol{s}_{01},\boldsymbol{s}_{02},\omega_1,\omega_2) & W_{yy}(\boldsymbol{r}_1,\boldsymbol{r}_2,\boldsymbol{s}_{01},\boldsymbol{s}_{02},\omega_1,\omega_2) \end{bmatrix}, \quad (13)$$

with $W_{\alpha\beta}^{(i)}(\boldsymbol{r}_1,\boldsymbol{r}_2,\boldsymbol{s}_{01},\boldsymbol{s}_{02},\omega_1,\omega_2) = \left[\left\langle E_\alpha^{(i)*}(\boldsymbol{r}_1,\boldsymbol{s}_{01},\omega_1)\, E_\beta^{(i)}(\boldsymbol{r}_2,\boldsymbol{s}_{02},\omega_2)\right\rangle\right]$, $(\alpha,\beta = x,y)$, which can be expressed in the following form:

$$W_{\alpha\beta}^{(i)}(\boldsymbol{r}_1,\boldsymbol{r}_2,\boldsymbol{s}_{01},\boldsymbol{s}_{02},\omega_1,\omega_2) = \iint\limits_{|\boldsymbol{s}_{01\perp}|^2\le 1} \iint\limits_{|\boldsymbol{s}_{02\perp}|^2\le 1} \mathrm{d}^2\boldsymbol{s}_{01\perp}\mathrm{d}^2\boldsymbol{s}_{02\perp} A_{\alpha\beta}(\boldsymbol{s}_{01\perp},\boldsymbol{s}_{02\perp},\omega_1,\omega_2) \exp\left[-\mathrm{i}\left(k_1\boldsymbol{s}_{01}\cdot\boldsymbol{r}_1 - k_2\boldsymbol{s}_{02}\cdot\boldsymbol{r}_2\right)\right], \quad (14)$$

where $\boldsymbol{s}_{0j\perp} = (p_j, q_j)$ $(j = 1, 2)$ is the projection of the unit vector $\boldsymbol{s}_0$ onto the source plane, and $k_j = \omega_j/c$ $(j = 1, 2)$ is the wave number with c being the speed of light in vacuum. It should be noted that in Eq. (13), the interval is chosen as $|\boldsymbol{s}_{0j\perp}|^2 \le 1$, indicating that the evanescent waves are omitted[7] and only the superposition of the electromagnetic pulsed waves in the electric field of the incident source is taken into consideration, and $A_{\alpha\beta}$ $(\boldsymbol{s}_{01\perp}, \boldsymbol{s}_{02\perp}, \omega_1, \omega_2)$ is an angular correlation function of an incident source, that is, the four-dimensional Fourier transform of the CSD matrix of the electric field components in the incident plane $z = 0$, and given by[7]

$$A_{\alpha\beta}(\boldsymbol{s}_{01\perp},\boldsymbol{s}_{02\perp},\omega_1,\omega_2) = \left(\frac{k_1k_2}{4\pi^2}\right)^2 \iint_{-\infty}^{\infty} \mathrm{d}^2\boldsymbol{\rho}_1\mathrm{d}^2\boldsymbol{\rho}_2 W_{\alpha\beta}^{(0)}(\boldsymbol{\rho}_1,\boldsymbol{\rho}_2,\omega_1,\omega_2) \times \exp\left[-\mathrm{i}\left(k_2\boldsymbol{s}_{02\perp}\cdot\boldsymbol{\rho}_2 - k_1\boldsymbol{s}_{01\perp}\cdot\boldsymbol{\rho}_1\right)\right]. \quad (15)$$

When equation (5) is substituted into Eq. (15), one obtains

$$A_{\alpha\beta}(\boldsymbol{s}_{01\perp},\boldsymbol{s}_{02\perp},\omega_1,\omega_2) = \frac{A_\alpha A_\beta B_{\alpha\beta} T_0}{2\pi\Omega_{0\alpha\beta}} \left(\frac{k_1k_2}{2\pi}\right)^2 w_0^2\sigma_{\alpha\beta}^2 \exp[-T_{\alpha\beta}(\omega_1,\omega_2)] \times \exp\left[-\frac{w_0^2\left(k_1\boldsymbol{s}_{01\perp} - k_2\boldsymbol{s}_{02\perp}\right)^2}{2} - \frac{\sigma_{\alpha\beta}^2\left(k_1\boldsymbol{s}_{01\perp} + k_2\boldsymbol{s}_{02\perp}\right)^2}{8}\right], \quad (16)$$

where

$$\frac{1}{\sigma_{\alpha\beta}^2} = \frac{1}{4w_0^2} + \frac{1}{\delta_{\alpha\beta}^2}. \quad (17)$$

In this research, we assume that the interaction between the incident source and the scatterer is extremely weak. Thus the first-order Born approximation is used to describe the scattering process.[1] Then the scattered wave $\boldsymbol{E}^{(s)}(r\boldsymbol{s},\omega)$ in the far-zone can be expressed as[2]

$$\boldsymbol{E}^{(s)}(r\boldsymbol{s},\omega) = -\boldsymbol{s}\times\left[\boldsymbol{s}\times\int_D F(\boldsymbol{r}',\omega)\boldsymbol{E}^{(i)}(\boldsymbol{r}',\boldsymbol{s}_0,\omega)G(r\boldsymbol{s},\boldsymbol{r}',\omega)\mathrm{d}^3\boldsymbol{r}'\right], \quad (18)$$

where $\boldsymbol{r}$ is the position vector of any point in the inside or outside space of the scatterer, $\boldsymbol{s} = (s_x, s_y, s_z)$ is the unit vector along a specified scattering path, and D denotes the scattered domain. $F(\boldsymbol{r}',\omega)$ is the scattering potential of the medium, and $G(r\boldsymbol{s},\boldsymbol{r}',\omega)$ is Green's function in free space, which can be given by[2]

$$G(r\boldsymbol{s},\boldsymbol{r}',\omega) = \frac{\exp(\mathrm{i}kr)}{r}\exp[-\mathrm{i}k\boldsymbol{s}\cdot\boldsymbol{r}']. \quad (19)$$

Based on Eq. (18), the three Cartesian coordinate components of the far-zero scattered field are written as

$$E_x^{(s)}(r\boldsymbol{s},\omega)=\int_D F(\boldsymbol{r}',\omega)G(r\boldsymbol{s},\boldsymbol{r}',\omega)\left[\left(1-s_x^2\right)E_x^{(i)}(\boldsymbol{r}',\boldsymbol{s}_0,\omega)-s_xs_yE_y^{(i)}(\boldsymbol{r}',\boldsymbol{s}_0,\omega)\right]\mathrm{d}^3\boldsymbol{r}', \tag{20a}$$

$$E_y^{(s)}(r\boldsymbol{s},\omega)=\int_D F(\boldsymbol{r}',\omega)G(r\boldsymbol{s},\boldsymbol{r}',\omega)\left[-s_xs_yE_x^{(i)}(\boldsymbol{r}',\boldsymbol{s}_0,\omega)-\left(1-s_y^2\right)E_y^{(i)}(\boldsymbol{r}',\boldsymbol{s}_0,\omega)\right]\mathrm{d}^3\boldsymbol{r}', \tag{20b}$$

$$E_z^{(s)}(r\boldsymbol{s},\omega)=\int_D F(\boldsymbol{r}',\omega)G(r\boldsymbol{s},\boldsymbol{r}',\omega)\left[-s_xs_zE_x^{(i)}(\boldsymbol{r}',\boldsymbol{s}_0,\omega)-s_ys_zE_y^{(i)}(\boldsymbol{r}',\boldsymbol{s}_0,\omega)\right]\mathrm{d}^3\boldsymbol{r}', \tag{20c}$$

where s_x, s_y, s_z are the three Cartesian coordinate components of the scattering direction $\boldsymbol{s}$. In addition, from Eq. (18), it is easy to find $\boldsymbol{s}\cdot E^{(s)}(r\boldsymbol{s},\omega)=0$. In other words, the electric field direction and the scattered wave vector direction are perpendicular to each other in the far-zero field. Thus, it is convenient to describe the scattered field in the spherical coordinate system. Hence, the radial component disappears, and only the remaining two non-zero components need considering. Moreover, the two non-zero components of the far-zero scattered field in the spherical coordinate system can be expressed as

$$\begin{aligned}E_\theta^{(s)}(r\boldsymbol{s},\omega)=&\cos\theta\cos\varphi E_x^{(s)}(r\boldsymbol{s},\omega)+\cos\theta\sin\varphi E_y^{(s)}(r\boldsymbol{s},\omega)\\&-\sin\theta E_z^{(s)}(r\boldsymbol{s},\omega),\end{aligned} \tag{21a}$$

$$E_\varphi^{(s)}(r\boldsymbol{s},\omega)=-\sin\varphi E_x^{(s)}(r\boldsymbol{s},\omega)+\cos\varphi E_y^{(s)}(r\boldsymbol{s},\omega), \tag{21b}$$

where θ is the scattering angle and φ is the observation azimuth. When equation (20) is substituted into Eq. (21), one obtains

$$\begin{aligned}E_\theta^{(s)}(r\boldsymbol{s},\omega)=&\int_D \mathrm{d}^3\boldsymbol{r}'F(\boldsymbol{r}',\omega)G(r\boldsymbol{s},\boldsymbol{r}',\omega)\\&\times\left[\cos\theta\cos\varphi E_x^{(i)}(\boldsymbol{r}',\boldsymbol{s}_0,\omega)\right.\\&\left.+\cos\theta\sin\varphi E_y^{(i)}(\boldsymbol{r}',\boldsymbol{s}_0,\omega)\right],\end{aligned} \tag{22a}$$

$$\begin{aligned}E_\varphi^{(s)}(r\boldsymbol{s},\omega)=&\int_D F(\boldsymbol{r}',\omega)G(r\boldsymbol{s},\boldsymbol{r}',\omega)\\&\times\left[-\sin\varphi E_x^{(i)}(\boldsymbol{r}',\boldsymbol{s}_0,\omega)\right.\\&\left.+\cos\varphi E_y^{(i)}(\boldsymbol{r}',\boldsymbol{s}_0,\omega)\right]\mathrm{d}^3\boldsymbol{r}',\end{aligned} \tag{22b}$$

where $s_x=\sin\theta\cos\varphi$, $s_y=\sin\theta\sin\varphi$, and $s_z=\cos\theta$.

Similarly, the CSD matrix of the scattered beam in the far-zero field is given by

$$\begin{aligned}&\boldsymbol{W}^{(s)}(r\boldsymbol{s}_1,r\boldsymbol{s}_2,\omega_1,\omega_2)\\=&\left[W_{\alpha\beta}^{(s)}(r\boldsymbol{s}_1,r\boldsymbol{s}_2,\omega_1,\omega_2)\right]\\=&\left[\left\langle E_\alpha^{(s)*}(r\boldsymbol{s}_1,\omega_1)\,E_\beta^{(s)}(r\boldsymbol{s}_2,\omega_2)\right\rangle\right],\\&(\alpha,\beta=\theta,\varphi).\end{aligned} \tag{23}$$

By substituting Eq. (22) into Eq. (23), and using Eqs. (14), (16), and (19), we can obtain the elements of the CSD matrix in the spherical coordinate system of a scattered partially polarized spatially and spectrally partially coherent EGSMP beam in the far-zero field, irradiating on a deterministic scattering medium, which are expressed as

$$\begin{aligned}&W_{\theta\theta}^{(s)}(r\boldsymbol{s}_1,r\boldsymbol{s}_2,\omega_1,\omega_2)\\=&\frac{\mathrm{e}^{[-\mathrm{i}(k_1-k_2)r]}}{r^2}[\cos\theta_1\cos\varphi_1\cos\theta_2\cos\varphi_2F_{xx}(r\boldsymbol{s}_1,r\boldsymbol{s}_2,\omega_1,\omega_2)\\&+\cos\theta_1\cos\varphi_1\cos\theta_2\sin\varphi_2F_{xy}(r\boldsymbol{s}_1,r\boldsymbol{s}_2,\omega_1,\omega_2)\\&+\cos\theta_1\sin\varphi_1\cos\theta_2\cos\varphi_2F_{yx}(r\boldsymbol{s}_1,r\boldsymbol{s}_2,\omega_1,\omega_2)\\&+\cos\theta_1\sin\varphi_1\cos\theta_2\sin\varphi_2F_{yy}(r\boldsymbol{s}_1,r\boldsymbol{s}_2,\omega_1,\omega_2)],\end{aligned} \tag{24a}$$

$$\begin{aligned}&W_{\theta\varphi}^{(s)}(r\boldsymbol{s}_1,r\boldsymbol{s}_2,\omega_1,\omega_2)\\=&\frac{\mathrm{e}^{[-\mathrm{i}(k_1-k_2)r]}}{r^2}[-\cos\theta_1\cos\varphi_1\sin\varphi_2F_{xx}(r\boldsymbol{s}_1,r\boldsymbol{s}_2,\omega_1,\omega_2)\\&+\cos\theta_1\cos\varphi_1\cos\varphi_2F_{xy}(r\boldsymbol{s}_1,r\boldsymbol{s}_2,\omega_1,\omega_2)\\&-\cos\theta_1\sin\varphi_1\sin\varphi_2F_{yx}(r\boldsymbol{s}_1,r\boldsymbol{s}_2,\omega_1,\omega_2)\\&+\cos\theta_1\sin\varphi_1\cos\varphi_2F_{yy}(r\boldsymbol{s}_1,r\boldsymbol{s}_2,\omega_1,\omega_2)],\end{aligned} \tag{24b}$$

$$\begin{aligned}&W_{\varphi\theta}^{(s)}(r\boldsymbol{s}_1,r\boldsymbol{s}_2,\omega_1,\omega_2)\\=&\frac{\mathrm{e}^{[-\mathrm{i}(k_1-k_2)r]}}{r^2}[-\sin\varphi_1\cos\theta_2\cos\varphi_2F_{xx}(r\boldsymbol{s}_1,r\boldsymbol{s}_2,\omega_1,\omega_2)\\&-\sin\varphi_1\cos\theta_2\sin\varphi_2F_{xy}(r\boldsymbol{s}_1,r\boldsymbol{s}_2,\omega_1,\omega_2)\\&+\cos\varphi_1\cos\theta_2\cos\varphi_2F_{yx}(r\boldsymbol{s}_1,r\boldsymbol{s}_2,\omega_1,\omega_2)\\&+\cos\varphi_1\cos\theta_2\sin\varphi_2F_{yy}(r\boldsymbol{s}_1,r\boldsymbol{s}_2,\omega_1,\omega_2)],\end{aligned} \tag{24c}$$

$$\begin{aligned}&W_{\varphi\varphi}^{(s)}(r\boldsymbol{s}_1,r\boldsymbol{s}_2,\omega_1,\omega_2)\\=&\frac{\mathrm{e}^{[-\mathrm{i}(k_1-k_2)r]}}{r^2}[\sin\varphi_1\sin\varphi_2F_{xx}(r\boldsymbol{s}_1,r\boldsymbol{s}_2,\omega_1,\omega_2)\\&-\sin\varphi_1\cos\varphi_2F_{xy}(r\boldsymbol{s}_1,r\boldsymbol{s}_2,\omega_1,\omega_2)\\&-\cos\varphi_1\sin\varphi_2F_{yx}(r\boldsymbol{s}_1,r\boldsymbol{s}_2,\omega_1,\omega_2)\\&+\cos\varphi_1\cos\varphi_2F_{yy}(r\boldsymbol{s}_1,r\boldsymbol{s}_2,\omega_1,\omega_2)].\end{aligned} \tag{24d}$$

Here,

$$\begin{aligned}&F_{\alpha\beta}(r\boldsymbol{s}_1,r\boldsymbol{s}_2,\omega_1,\omega_2)\\=&\iint\limits_{|\boldsymbol{s}_{01\perp}|^2\le1}\iint\limits_{|\boldsymbol{s}_{01\perp}|^2\le1}\tilde{F}^*(\boldsymbol{K}_1,\omega_1)\tilde{F}(\boldsymbol{K}_2,\omega_2)\\&\times A_{\alpha\beta}(\boldsymbol{s}_{01\perp},\boldsymbol{s}_{02\perp},\omega_1,\omega_2)\mathrm{d}^3\boldsymbol{s}_{01\perp}\mathrm{d}^3\boldsymbol{s}_{02\perp},\\&(\alpha,\beta=x,y),\end{aligned} \tag{25}$$

where $A_{\alpha\beta}(\boldsymbol{s}_{01\perp},\ \boldsymbol{s}_{02\perp},\ \omega_1,\ \omega_2)$ is shown in Eq. (16), and $\boldsymbol{K}_j=k_j(\boldsymbol{s}_j\boldsymbol{s}_{0j})$ $(j=1,2)$ is a vector. Here,

$$\tilde{F}(\boldsymbol{K},\omega)=\int_D F(\boldsymbol{r}',\omega)\exp[-\mathrm{i}\boldsymbol{K}\cdot\boldsymbol{r}']\mathrm{d}^3\boldsymbol{r}' \tag{26}$$

is the three-dimensional Fourier transform of the scattering potential $F(\boldsymbol{r}',\omega)$. Let $n(\boldsymbol{r}',\omega)$ be the refractive index dis-

tribution throughout the scatterer, then the scattering potential $F(\boldsymbol{r}',\omega)$ will be given by the following formula:[25,26]

$$F(\boldsymbol{r}',\omega)=\begin{cases}\dfrac{k^2}{4\pi}\left[n^2(\boldsymbol{r}',\omega)-1\right], & \boldsymbol{r}'\in D,\\ 0, & \text{otherwise.}\end{cases} \tag{27}$$

In this research we assume that there is a deterministic medium with a three-dimensional Gaussian distribution scattering potential, *i.e.*[7]

$$F(\boldsymbol{r}',\omega)=F_0\exp\left[-\frac{\boldsymbol{r}'^2}{2\sigma_R^2}\right], \tag{28}$$

where F_0 is a positive constant, σ_R is the effective width of the medium,[25] and the beam condition is satisfied, *i.e.*, $\sigma_R\gg\lambda_0/\pi\sqrt{2}$.[26] In this case, by substituting Eq. (28) into Eq. (26), one obtains

$$\begin{aligned}&\tilde{F}^*(\boldsymbol{K}_1,\omega_1)\tilde{F}(\boldsymbol{K}_2,\omega_2)\\ &=\int_D\int_D F^*(\boldsymbol{r}_1',\omega_1)F(\boldsymbol{r}_2',\omega_2)\\ &\quad\times\exp\left[\mathrm{i}\left(\boldsymbol{K}_1\cdot\boldsymbol{r}_1'-\boldsymbol{K}_2\cdot\boldsymbol{r}_2'\right)\right]\mathrm{d}^3\boldsymbol{r}_1'\,\mathrm{d}^3\boldsymbol{r}_2'\\ &=F_0^2(2\pi)^3\sigma_R^6\exp\left[-\frac{\sigma_R^2}{2}\left(\boldsymbol{K}_1^2+\boldsymbol{K}_2^2\right)\right].\end{aligned} \tag{29}$$

when equations (16) and (29) are substituted into Eq. (25), one obtains

$$\begin{aligned}&F_{\alpha\beta}(r\boldsymbol{s}_1,r\boldsymbol{s}_2,\omega_1,\omega_2)\\ &=\frac{k_1^2k_2^2A_\alpha A_\beta B_{\alpha\beta}T_0F_0^2\sigma_R^6w_0^2\sigma_{\alpha\beta}^2}{\Omega_{0\alpha\beta}}\exp[-T_{\alpha\beta}(\omega_1,\omega_2)]\\ &\times\iint\limits_{p_1^2+q_1^2\le1}\iint\limits_{p_2^2+q_2^2\le1}\exp\left\{-\frac{\sigma_R^2k_1^2}{2}(s_{1x}-p_1)^2+(s_{1y}-q_1)^2+\left(s_{1z}-\sqrt{1-p_1^2-q_1^2}\right)^2\right\}\\ &\times\exp\left\{-\frac{\sigma_R^2k_2^2}{2}(s_{2x}-p_2)^2+(s_{2y}-q_2)^2+\left(s_{2z}-\sqrt{1-p_2^2-q_2^2}\right)^2\right\}\\ &\times\exp\left\{-\frac{w_0^2}{2}\left[k_1^2(p_1^2+q_1^2)-2k_1k_2(p_1p_2+q_1q_2)+k_2^2(p_2^2+q_2^2)\right]\right\}\\ &\times\exp\left\{-\frac{\sigma_{\alpha\beta}^2}{8}\left[k_1^2(p_1^2+q_1^2)+2k_1k_2(p_1p_2+q_1q_2)+k_2^2(p_2^2+q_2^2)\right]\right\}\mathrm{d}p_1\,\mathrm{d}q_1\,\mathrm{d}p_2\,\mathrm{d}q_2,\quad(\alpha,\beta=x,y),\end{aligned} \tag{30}$$

where $\boldsymbol{s}_1=(s_{1x},s_{1y},s_{1z}),\boldsymbol{s}_2=(s_{2x},s_{2y},s_{2z})$.

To derive the integral in Eq. (30), we have used an approach similar to that shown in Ref. [8]. It is clearly seen that in Eq. (16), the value of the $A_{\alpha\beta}(\boldsymbol{s}_{01\perp},\boldsymbol{s}_{02\perp},\omega_1,\omega_2)$ declines exponentially with the increase of p_1, q_1, and p_2, q_2. Thus, it is assumed that

i) only the values within the interval of $p_1^2+q_1^2\ll1$ and $p_2^2+q_2^2\ll1$ have a significant influence on the integral;

ii) the value of the angular correlation function is zero unless $p_1^2+q_1^2\ll1$ and $p_2^2+q_2^2\ll1$, so the integral range can be extended to ∞.

Furthermore, under the circumstance, $\sqrt{1-p_1^2-q_1^2}$ and $\sqrt{1-p_2^2-q_2^2}$ may be given in the first-order approximation of the Taylor expansion as $1-(p_1^2+q_1^2)/2$ and $1-(p_2^2+q_2^2)/2$, respectively.[8]

After extensive integral calculations, $F_{\alpha\beta}(r\boldsymbol{s}_1,r\boldsymbol{s}_2,\omega_1,\omega_2)$ in Eq. (30) can be written as

$$\begin{aligned}&F_{\alpha\beta}(r\boldsymbol{s}_1,r\boldsymbol{s}_2,\omega_1,\omega_2)\\ &=\frac{k_1^2k_2^2A_\alpha A_\beta B_{\alpha\beta}T_0F_0^2\sigma_R^6w_0^2\sigma_{\alpha\beta}^2}{\Omega_{0\alpha\beta}}\exp[-T_{\alpha\beta}(\omega_1,\omega_2)]\\ &\times\frac{\pi^2}{m_{2\alpha\beta}n_{\alpha\beta}}\exp\left[\frac{k_2^2\sigma_R^4(s_{2x}^2+s_{2y}^2)}{4m_{2\alpha\beta}}+\frac{\xi_{x\alpha\beta}^2+\xi_{y\alpha\beta}^2}{4n_{\alpha\beta}}\right]\\ &\times\exp\left\{-\sigma_R^2\left[k_1^2(1-s_{1z})+k_2^2(1-s_{2z})\right]\right\},\\ &(\alpha,\beta=x,y),\end{aligned} \tag{31}$$

where

$$\begin{aligned}a_{\alpha\beta}&=\frac{w_0^2}{2}+\frac{\sigma_{\alpha\beta}^2}{8},\quad b_{\alpha\beta}=\frac{w_0^2}{2}-\frac{\sigma_{\alpha\beta}^2}{8},\\ m_{j\alpha\beta}&=k_j^2a_{\alpha\beta}+k_j^2\frac{\sigma_R^2}{2}s_{jz}\quad(j=1,2),\\ n_{\alpha\beta}&=m_{1\alpha\beta}-\frac{k_1^2k_2^2b_{\alpha\beta}^2}{m_{2\alpha\beta}},\\ \xi_{x\alpha\beta}&=k_1^2\sigma_R^2s_{1x}+\frac{k_1k_2^3\sigma_R^2b_{\alpha\beta}}{m_{2\alpha\beta}}s_{2x},\\ \xi_{y\alpha\beta}&=k_1^2\sigma_R^2s_{1y}+\frac{k_1k_2^3\sigma_R^2b_{\alpha\beta}}{m_{2\alpha\beta}}s_{2y}.\end{aligned} \tag{32}$$

Therefore, the statistical properties of far-zone scattered field can be given by the average spectral intensity

$$S(r\boldsymbol{s},\omega)=W_{\theta\theta}^{(s)}(r\boldsymbol{s},r\boldsymbol{s},\omega,\omega)+W_{\varphi\varphi}^{(s)}(r\boldsymbol{s},r\boldsymbol{s},\omega,\omega), \tag{33}$$

the spectral degree of polarization (DOP) is

$$P(\boldsymbol{rs},\omega) = \sqrt{1-\frac{4\mathrm{Det}\boldsymbol{W}^{(s)}(\boldsymbol{rs},\boldsymbol{rs},\omega,\omega)}{\mathrm{Tr}^2\boldsymbol{W}^{(s)}(\boldsymbol{rs},\boldsymbol{rs},\omega,\omega)}} = \frac{\sqrt{\left(W^{(s)}_{\theta\theta}-W^{(s)}_{\varphi\varphi}\right)^2+4W^{(s)}_{\theta\varphi}W^{(s)}_{\varphi\theta}}}{W^{(s)}_{\theta\theta}+W^{(s)}_{\varphi\varphi}}, \quad (34)$$

and the spectral DOC is

$$\mu(\boldsymbol{rs}_1,\boldsymbol{rs}_2,\omega_1,\omega_2) = \frac{\sqrt{\mathrm{tr}\left[\boldsymbol{W}^{(s)}(\boldsymbol{rs}_1,\boldsymbol{rs}_2,\omega_1,\omega_2)\boldsymbol{W}^{(s)*}(\boldsymbol{rs}_1,\boldsymbol{rs}_2,\omega_1,\omega_2)\right]}}{\sqrt{\boldsymbol{S}(\boldsymbol{rs}_1,\omega_1)\boldsymbol{S}(\boldsymbol{rs}_2,\omega_2)}}. \quad (35)$$

It should be noted that equation (35) describes the two-frequency, two-point spectral DOC in the space–frequency domain. In practical terms, for the non-stationary fields, the field correlations between different frequencies at one specified space position $\boldsymbol{rs}_1=\boldsymbol{rs}_2=\boldsymbol{rs}$ may be of greater interest.[27] Therefore, in the paper we will use the term "spectral coherence" to describe the correlation properties between the spectral components rather than to depict the spatial coherence studied in the space frequency domain.[26] Under this circumstance, equation (30) is expressed as

$$\begin{aligned} &F_{\alpha\beta}(\boldsymbol{rs},\boldsymbol{rs},\omega_1,\omega_2) \\ &= \frac{A_\alpha A_\beta B_{\alpha\beta}T_0F_0^2\sigma_R^6w_0^2\sigma_{\alpha\beta}^2}{\Omega_{0\alpha\beta}}\exp[-T_{\alpha\beta}(\omega_1,\omega_2)] \\ &\times\frac{\pi^2}{m_{\alpha\beta}n_{\alpha\beta}}\exp\left[\left(\frac{\sigma_R^4}{4m_{\alpha\beta}}+\frac{\mu_{\alpha\beta}^2}{4n_{\alpha\beta}}\right)(s_x^2+s_y^2)\right] \\ &\times\exp\left[-\sigma_R^2\left(k_1^2+k_2^2\right)(1-s_z)\right], \\ &(\alpha,\beta=x,y), \end{aligned} \quad (36)$$

with

$$\begin{aligned} &a_{\alpha\beta}=\frac{w_0^2}{2}+\frac{\sigma_{\alpha\beta}^2}{8},\quad b_{\alpha\beta}=\frac{w_0^2}{2}-\frac{\sigma_{\alpha\beta}^2}{8}, \\ &\mu_{\alpha\beta}=k_1^2\sigma_R^2+\frac{k_1k_2^3\sigma_R^2b_{\alpha\beta}}{m_{\alpha\beta}}, \\ &m_{\alpha\beta}=a_{\alpha\beta}+\frac{\sigma_R^2}{2}s_z,\quad n_{\alpha\beta}=m_{\alpha\beta}-\frac{k_2^2b_{\alpha\beta}^2}{m_{\alpha\beta}}. \end{aligned} \quad (37)$$

When equations (36) and (37) are substituted into Eq. (35), the degree of spectral coherence $\mu(\boldsymbol{rs},\omega_1,\omega_2)$ of a scattered partially polarized spatially and spectrally partially coherent EGSMP beam can be obtained.

3. Numerical simulations and discussion

Now, we use Eqs. (7)–(12) and Eqs. (33)–(35) to graphically investigate the behaviors of the statistical properties of the incident field and the far-zero scattered field. Several relevant parameters are selected when a partially polarized spatially and spectrally partially coherent EGSMP beam is incident on a deterministic medium. The calculation parameters are shown in Table 1, unless otherwise specified. We employ the parameters as examples for the numerical simulations. Other values could also be used depending on the situations. Moreover, all of the parameters satisfy the following beam conditions[22]

$$\begin{cases} \dfrac{1}{4w_0^2}+\dfrac{1}{\delta_{\alpha\alpha}^2}\le\dfrac{2\pi^2}{\lambda^2},\ (\alpha=x,y),\sigma_R\gg\dfrac{\lambda_0}{\pi\sqrt{2}}, \\ \max\left\{\delta_{xx},\delta_{yy}\right\}\le\delta_{xy}\le\min\left\{\dfrac{\delta_{xx}}{|B_{xy}|},\dfrac{\delta_{yy}}{|B_{xy}|}\right\}, \\ \max\left\{T_{cxx},T_{cyy}\right\}\le T_{cxy}\le\min\left\{\dfrac{T_{cxx}}{|B_{xy}|},\dfrac{T_{cyy}}{|B_{xy}|}\right\}. \end{cases} \quad (38)$$

Table 1. Simulation parameters.

Parameter	Simulation value	Unit
Wavelength λ_0	632.8	nm
Beam width w_0	5	mm
Pulse duration T_0	5	fs
Spatial coherence width $\delta_{\alpha\beta}$	$\delta_{xx}=1$, $\delta_{yy}=0.5\delta_{xx}$, $\delta_{xy}=\delta_{yx}=1.5\delta_{xx}$	mm
Temporal coherence width of the pulse $T_{c\alpha\beta}$	$T_{cxx}=5$, $T_{cyy}=0.5T_{cxx}$, $T_{cxy}=T_{cyx}=1.5T_{cxx}$	fs
Average amplitudes A_α	$A_x=1.5$, $A_y=1$	/
Correlation coefficient $B_{\alpha\beta}$	$B_{xx}=B_{yy}=1$, $B_{xy}=B_{yx}^*=0.3\exp(\mathrm{i}\pi/3)$	/
Effective width of the medium σ_R	$1.0\lambda_0$	nm
Observation azimuth φ	0	rad
Angular frequency ω	$\omega_0=3.0\times10^{15}$, $\omega=1.1\omega_0$, $\omega_1=1.05\omega_0$, $\omega_2=0.95\omega_0$	rad/s

Figure 2 depicts the contour graphs of the normalized spectral intensity $S(\boldsymbol{rs},\omega)/S_{\max}(\boldsymbol{rs},\omega)$ of a scattered partially polarized spatially and spectrally partially coherent EGSMP beam for different values of the effective width of the medium σ_R as a function of the scattering angle θ and observation angle φ, the pulse duration T_0 and the temporal coherence length T_{cxx}. It can

be clearly seen that all the σ_R, φ, and T_0 affect the distribution of the normalized spectral intensity $S(rs,\omega)/S_{\max}(rs,\omega)$, whereas T_{cxx} hardly influences its distribution. With the increase of σ_R, the profile of the normalized spectral intensity $S(rs,\omega)/S_{\max}(rs,\omega)$ quickly changes. For the case of the unaltered φ (see Figs. 2(b1)–2(b4)), $|\theta|$ corresponding to the value of $S(rs,\omega)/S_{\max}(rs,\omega)$ increases as T_0 grows. In addition, σ_R has a significant influence on the normalized spectral intensity of the far-zero scattered field.

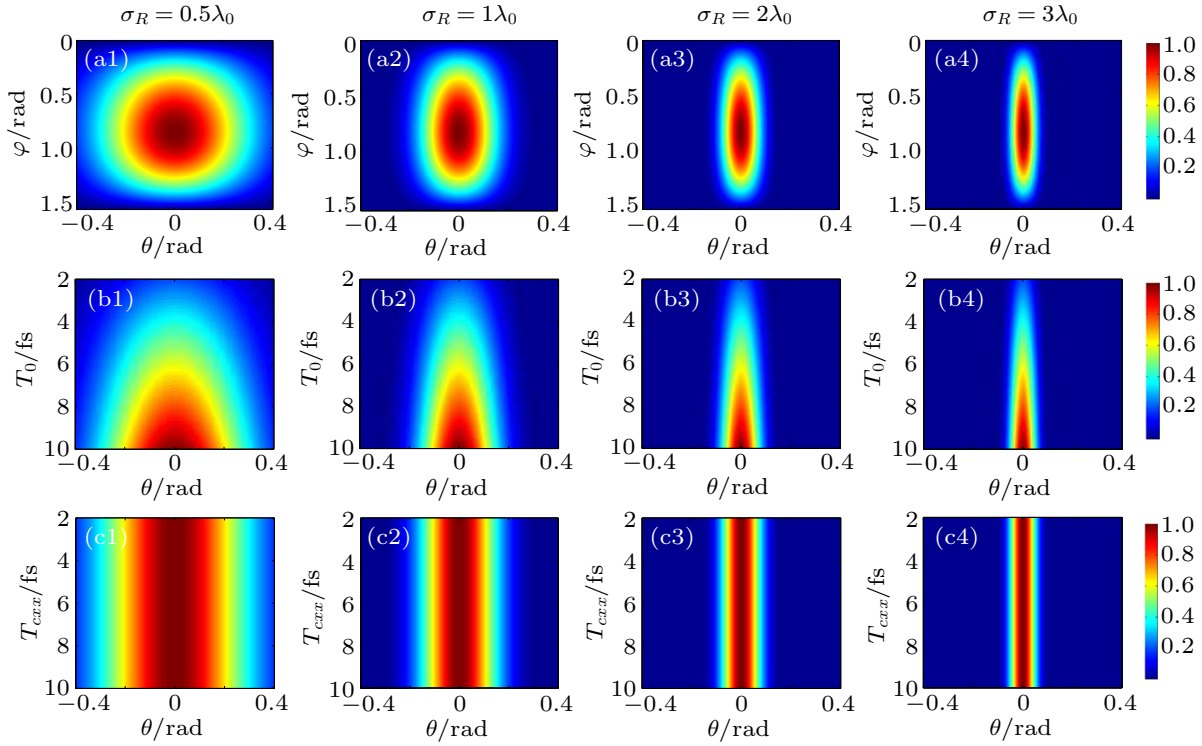

Fig. 2. Contour graphs of normalized spectral intensity of scattered partially polarized spatially and spectrally partially coherent EGSMP beam for different values of σ_R as a function of θ and [(a1)–(a4)] φ, [(b1)–(b4)] T_0, and [(c1)–(c4)] T_{cxx}.

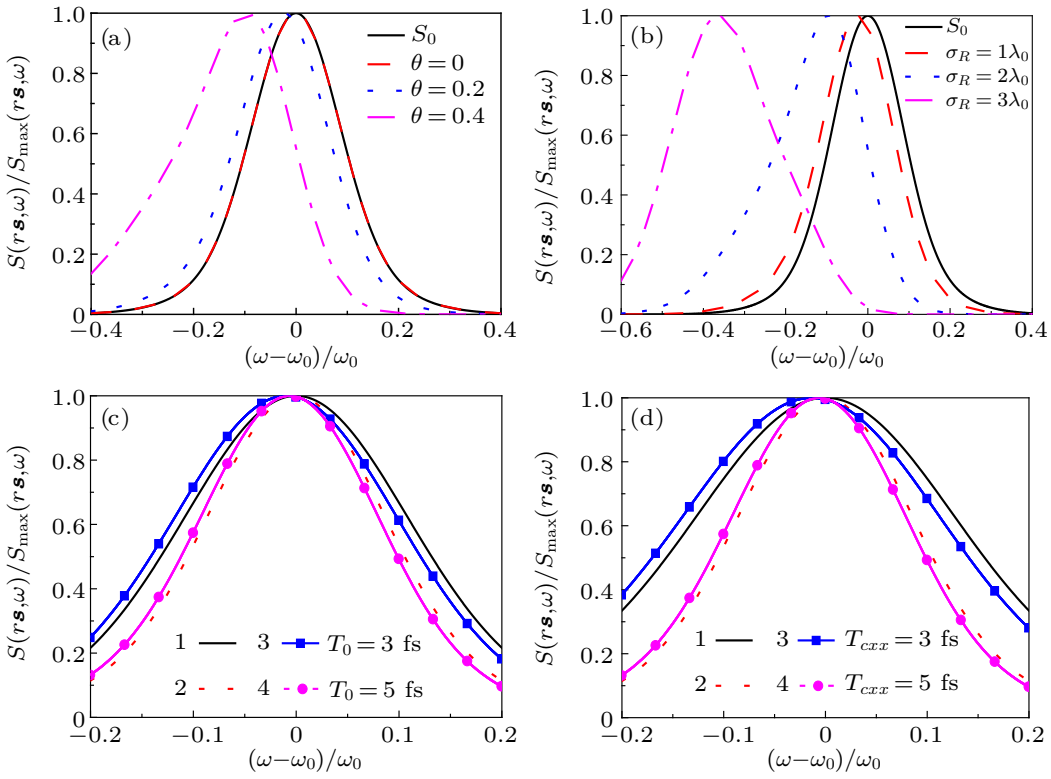

Fig. 3. Comparison between incident field and scattered field with respect to the normalized spectral intensity *versus* relative spectral shift $(\omega-\omega_0)/\omega_0$ for different values of (a) θ, (b) σ_R, (c) T_0, and (d) T_{cxx}, with [(a) and (b)] S_0 denoting incident normalized spectral intensity, [(c) and (d)] numbers 1 and 2 representing incident normalized spectral intensity, and 3 and 4 referring to scattered normalized spectral intensity.

Figure 3 shows the normalized spectral intensity $S(r\boldsymbol{s},\omega)/S_{\max}(r\boldsymbol{s},\omega)$ of both the incident and the scattered partially polarized spatially and spectrally partially coherent EGSMP beam *versus* the relative spectral shift $\delta\omega/\omega_0=(\omega-\omega_0)/\omega_0$ for different values of the scattering angle θ (see Fig. 3(a)), the effective width of the medium σ_R (see Fig.3(b)), the pulse duration T_0 (see Fig. 3(c)), and the temporal coherence length T_{cxx} (see Fig. 3(e)). Compared with the incident spectral intensity, it is found that the normalized spectral intensity shifts toward the smaller frequency, *i.e.*, a red shift occurs. The red shift increases as both θ and σ_R increase, and the red shift decreases as both T_0 and T_{cxx} increase. Moreover, the relative spectral width $|(\omega-\omega_0)/\omega_0|$ decreases with the increase of T_0 and T_{cxx}, which is defined as a corresponding relative spectral shift distance as the spectral intensity drops to its e^{-2} times.

Figure 4 shows the spectral DOPs of a scattered partially polarized spatially and spectrally partially coherent EGSMP beam *versus* the relative spectral shift $\delta\omega/\omega_0=(\omega-\omega_0)/\omega_0$ for different values of panels (a1, b1) the scattering angle θ, panels (b1, b2) the effective width of the medium σ_R, panels (c1, c2) the pulse duration T_0, panels (d1, d2) the temporal coherence length T_{cxx}, and the coefficients $B_{\alpha\beta}$. For panels (a1)–(d1) $B_{xy}=B_{yx}=0$, panels (a2)–(d2) $B_{xy}=B_{yx}^{*}=0.3\times\exp(\mathrm{i}\pi/3)$. It can be seen from Fig. 4 that the coefficients $B_{\alpha\beta}$ affects only the value of the spectral DOP, and they barely affect the distribution of the spectral DOP. For the case of the $\delta\omega/\omega_0=0$, the corresponding value of the spectral DOP decreases as both θ and T_{cxx} increase except for $\theta=\pi/2$, and the corresponding value increases as T_0 increases. In addition, the relative spectral width $|(\omega-\omega_0)/\omega_0|$ decreases as θ, T_0, and T_{cxx} all increase. It can be clearly seen that for $\theta=\pi/2$, the value of the spectral DOP is always kept at 1 for different values of the coefficients $B_{\alpha\beta}$. At the same time, it is found that the value of the spectral DOP remains invariant as σ_R varies. This implies that the behavior of the spectral DOP of the scattered partially polarized partially coherent EGSMP beam is independent of the value of σ_R.

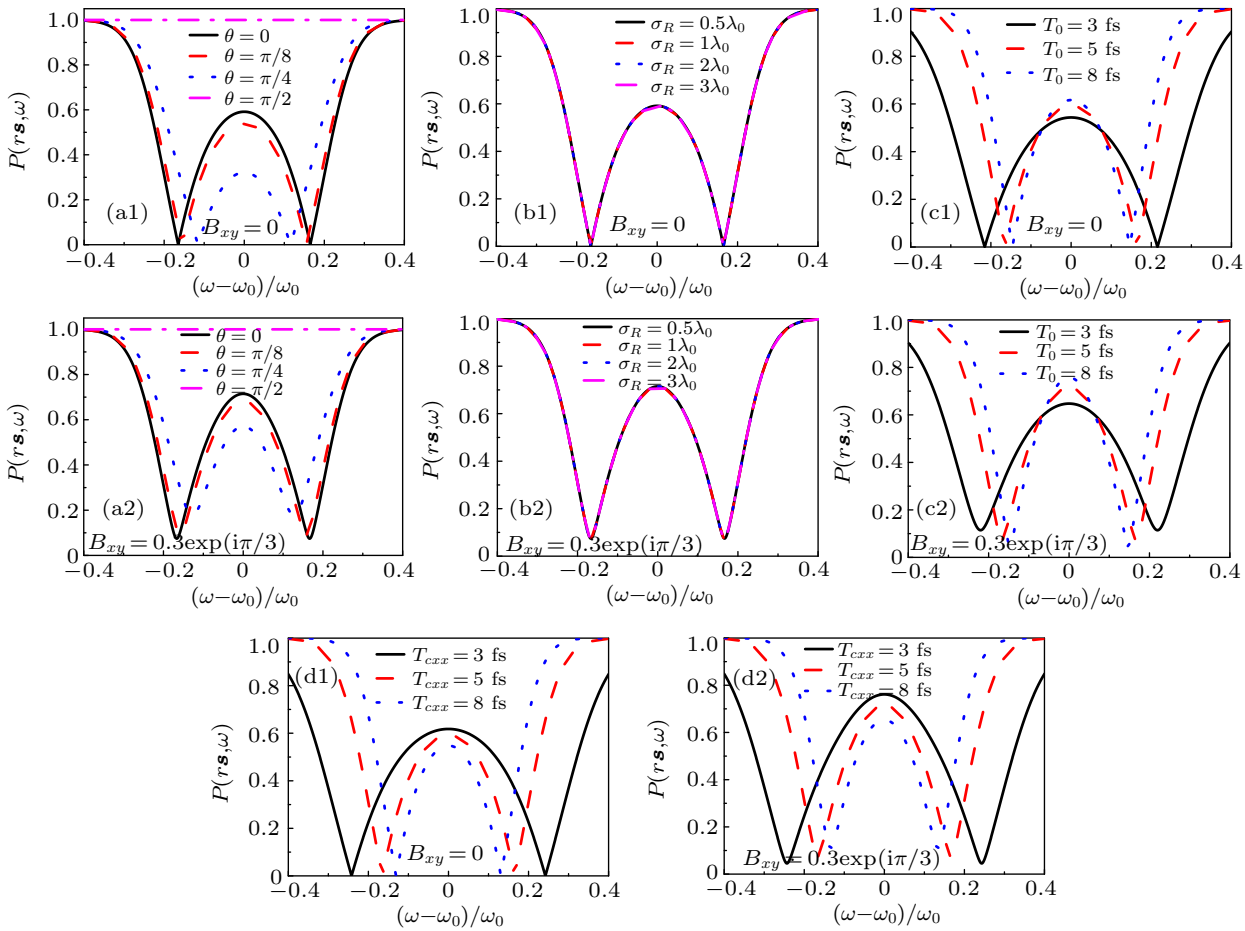

Fig. 4. Behaviors of the spectral DOP of scattered partially polarized spatially and spectrally partially coherent EGSMP beam *versus* relative spectral shift $(\omega-\omega_0)/\omega_0$ for different values of (a1, a2) θ, (b1, b2) σ_R, (c1, c2) T_0, and (d1, d2) T_{cxx}, with [(a1)–(d1)] $B_{xy}=B_{yx}=0$, and [(a2)–(d2)] $B_{xy}=B_{yx}^{*}=0.3\times\exp(\mathrm{i}\pi/3)$.

To learn more about the vector properties, the behaviors of the spectral DOPs of both the incident and scattered partially polarized partially coherent EGSMP beam *versus* the scattering angle θ for different values of the pulse duration T_0, the temporal

coherence length T_{cxx}, and the coefficients $B_{\alpha\beta}$ are shown in Fig. 5. It can clearly be seen that the coefficient $B_{\alpha\beta}$ has an influence only on the value of the spectral DOP, and it hardly affects the distribution of the spectral DOP. For the case of $\theta = 0$ or π, the value of the spectral DOP decreases as both the T_0 and T_{cxx} increase. As can be seen in Figs. 5(a2) and 5(b2), the minimum value of the spectral DOP decreases as both T_0 and T_{cxx} grow, and the maximum value of the spectral DOP stays constant as both T_0 and T_{cxx} vary. Moreover, the T_{cxx} exerts a more obvious effect on the spectral DOP. Comparing with the incident field, the spectral DOP of the scattered field varies periodically with position, and it is always less than the initial value for a certain distance. Otherwise, it is greater than the initial value. This implies that the state of polarization of scattered field can be changed by adjusting its position.

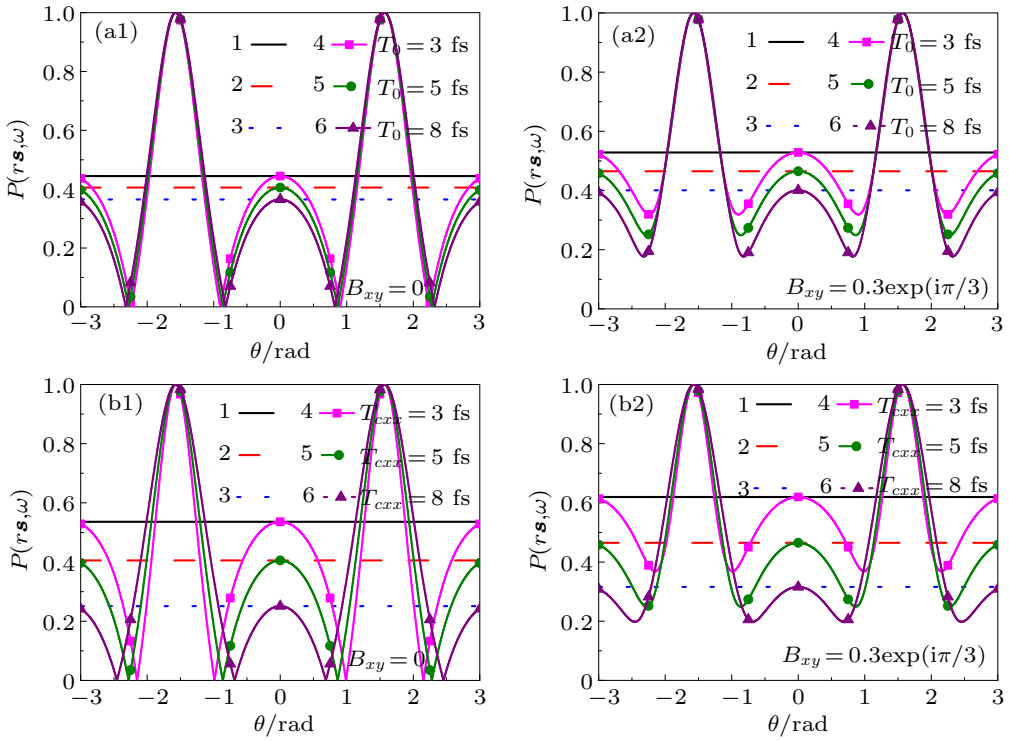

Fig. 5. Behaviors of spectral DOP of both incident and scattered partially polarized spatially and spectrally partially coherent EGSMP beam *versus* scattering angle θ for different values of [(a1),(a2)] T_0 and [(b1), (b2)] T_{cxx}, with [(a1), (b1)] $B_{xy} = B_{yx} = 0$, [(a2), (b2)] $B_{xy} = B_{yx}^* = 0.3 \times \exp(i\pi/3)$, numbers 1–3 denoting incident spectral DOP, and numbers 4–6 representing scattered spectral DOP.

The polarization properties, *i.e.*, the coherence properties of the scattered light field at a single point in terms of both space and frequency, are contained in the polarization matrix $\boldsymbol{J}^{(s)}(\boldsymbol{rs}, \omega)$. This matrix is defined as[28]

$$\boldsymbol{J}^{(s)}(\boldsymbol{rs}, \omega) = \boldsymbol{W}^{(s)}(\boldsymbol{rs}, \boldsymbol{rs}, \omega, \omega). \tag{39}$$

The spectral polarization matrix can be split into two parts, *i.e.*,

$$\boldsymbol{J}^{(s)}(\boldsymbol{rs}, \omega) = \boldsymbol{J}_u^{(s)}(\boldsymbol{rs}, \omega) + \boldsymbol{J}_p^{(s)}(\boldsymbol{rs}, \omega),$$

where the former represents a fully unpolarized field and the latter refers to a completely polarized field. The spectral degree of polarization $P(\boldsymbol{rs}, \omega)$, which is defined as the ratio of the intensity of the polarized component to the total intensity, at a point $\boldsymbol{rs}$ and frequency ω, is then obtained from the following expressions[28]

$$P^2(\boldsymbol{rs}, \omega) = 1 - \frac{\det \boldsymbol{J}^{(s)}(\boldsymbol{rs}, \omega)}{\mathrm{tr}^2\, \boldsymbol{J}^{(s)}(\boldsymbol{rs}, \omega)}$$

$$= 2\frac{\mathrm{tr}\, \boldsymbol{J}^{(s)2}(\boldsymbol{rs}, \omega)}{\mathrm{tr}^2\, \boldsymbol{J}^{(s)}(\boldsymbol{rs}, \omega)} - 1. \tag{40}$$

Like the conventional form, as shown in Eq. (37), the first equality shows a new expression for the spectral degree of polarization, while the second equality follows from the properties of the polarization matrix $\boldsymbol{J}^{(s)}(\boldsymbol{rs}, \omega)$.

Recalling the definition of the spectral degree of coherence $\mu(\boldsymbol{rs}_1, \boldsymbol{rs}_2, \omega_1, \omega_2)$, as shown in Eq. (36), it is of interest to find that

$$P^2(\boldsymbol{rs}, \omega) = 2\mu^2(\boldsymbol{rs}, \boldsymbol{rs}, \omega, \omega) - 1. \tag{41}$$

This equation establishes a connection between $P(\boldsymbol{rs}, \omega)$ and the equal-point value of the space–frequency domain spectral degree of coherence, $\mu(\boldsymbol{rs}, \boldsymbol{rs}, \omega, \omega)$. In other words, equation (41) implies that there is an intrinsic relationship between the spectral degree of coherence and the spectral degree of polarization of the scattered light field.

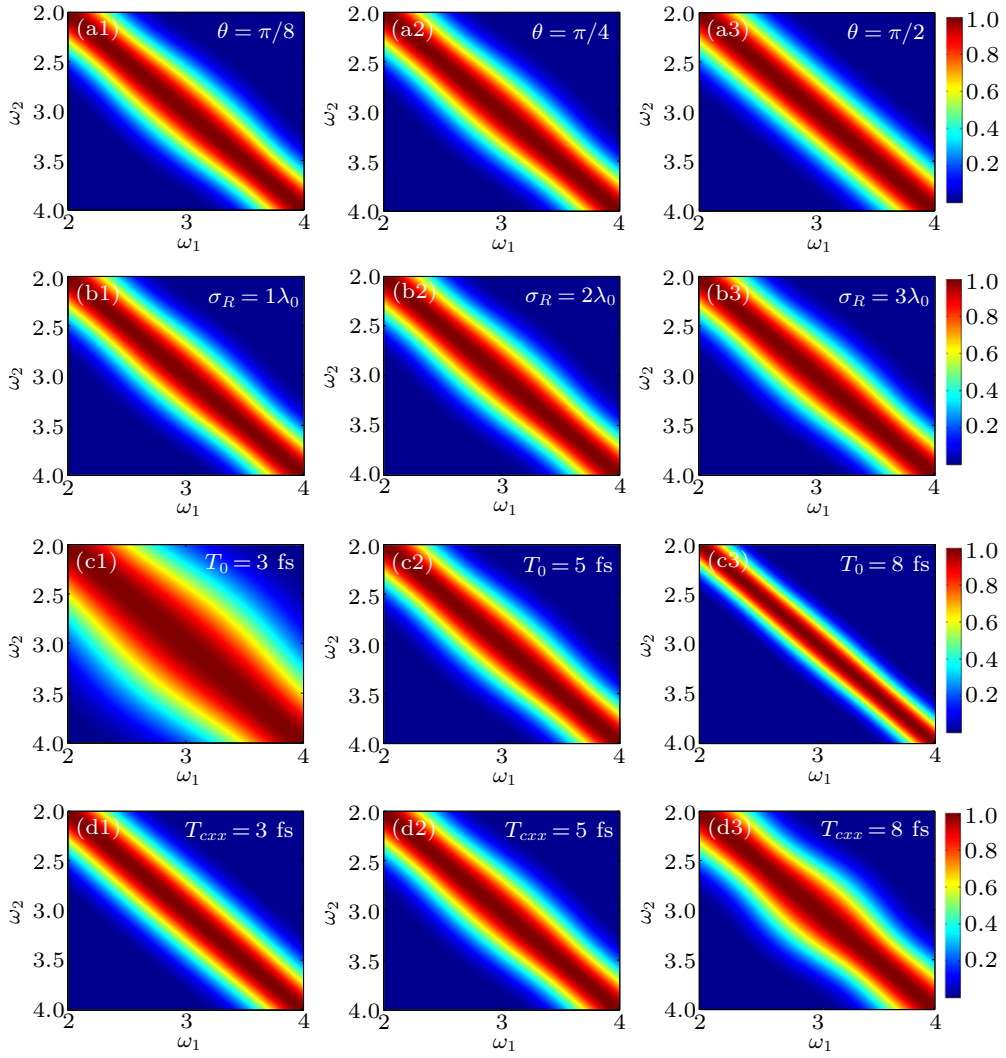

Fig. 6. Contour graphs of modulus of degree of spectral coherence of scattered partially polarized spatially and spectrally partially coherent EGSMP beam as a function of ω_1 and ω_2 for different values of θ, σ_R, T_0, and T_{cxx}.

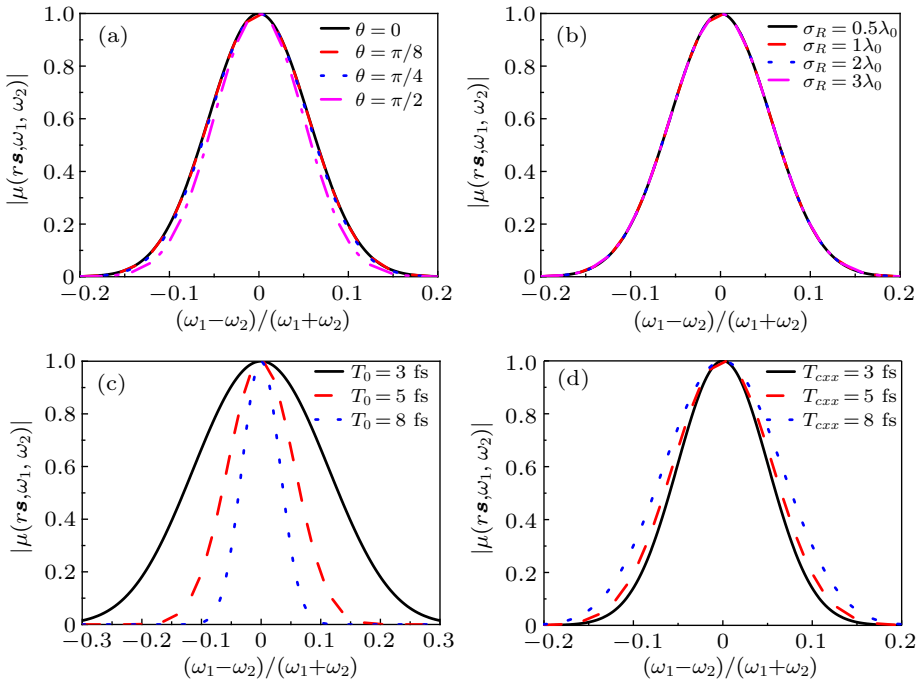

Fig. 7. Curves of modulus of degree of spectral coherence of scattered partially polarized spatially and spectrally partially coherent EGSMP beam *versus* $(\omega_1 - \omega_2)/(\omega_1 + \omega_2)$ for different values of θ, σ_R, T_0, and T_{cxx}.

Finally, we study the spectral coherence of a scattered partially polarized spatially and spectrally partially coherent EGSMP beam. Figure 6 illustrates the countour graphs of the modulus of the degree of spectral coherence $|\mu(rs,\omega_1,\omega_2)|$ as a function of ω_1 and ω_2 for different values of the scattering angle θ, the effective width of the medium σ_R, the pulse duration T_0, and the temporal coherence length T_{cxx}. To learn the behaviors of the spectral coherence, we also calculate the relations between modulus of the degree of spectral coherence $|\mu(rs,\omega_1,\omega_2)|$ and $(\omega_1-\omega_2)/(\omega_1+\omega_2)$ at different values of the scattering angle θ, the effective width of the medium σ_R, the pulse duration T_0 and the temporal coherence length T_{cxx} as shown in Fig. 7. It is found that the θ slightly affects the structure of $|\mu(rs,\omega_1,\omega_2)|$, whereas σ_R influences barely the distribution of $|\mu(rs,\omega_1,\omega_2)|$ as shown in Figs. 6(a1)–6(b3), and 7(a) and 7(b). At the same time, it can be clearly seen in Figs. 6(c1)–6(d3) and 7(c) and 7(d) that both T_0 and T_{cxx} significantly affect the structure of $|\mu(rs,\omega_1,\omega_2)|$, and the former's effect is greater. In addition, the relative spectral width decreases with T_0 rising and T_{cxx} dropping.

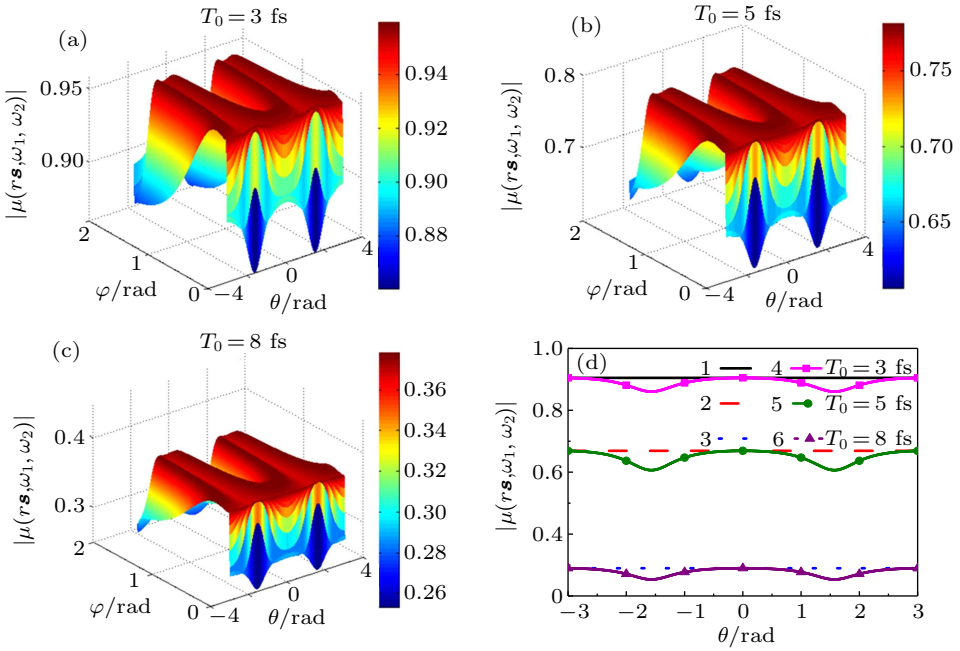

Fig. 8. The 3D moduli of degree of spectral coherence distribution and corresponding cross line ($\varphi=0$) of scattered partially polarized spatially and spectrally partially coherent EGSMP beam for different values of T_0, with numbers 1–3 denoting incident modulus of degree of spectral coherence, and numbers 4–6 referring to scattered modulus of degree of spectral coherence.

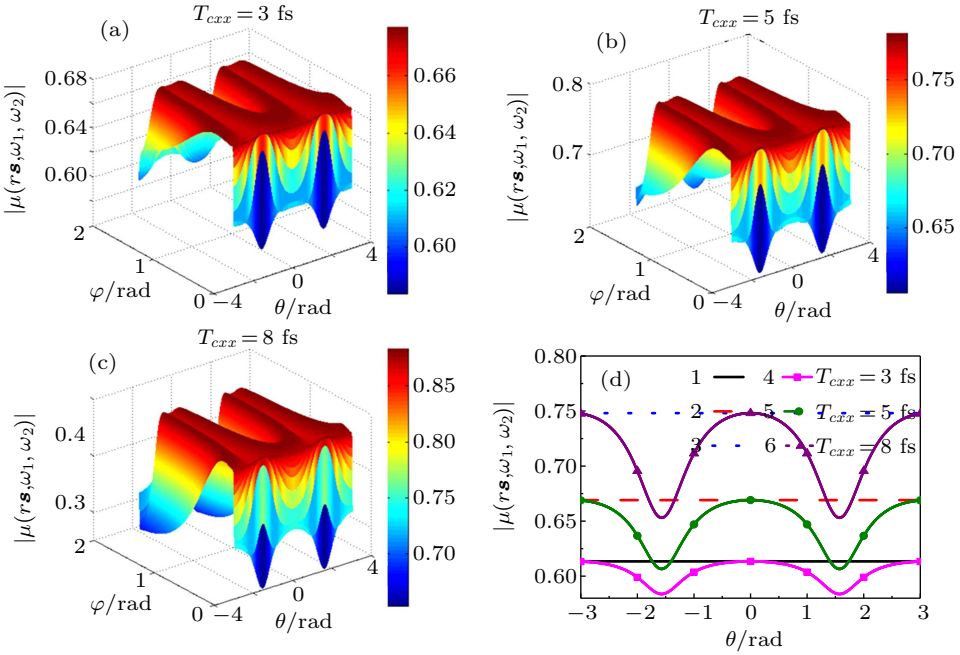

Fig. 9. 3D moduli of degree of spectral coherence distribution and corresponding cross line ($\varphi=0$) of scattered partially polarized spatially and spectrally partially coherent EGSMP beam for different values of T_{cxx}, with numbers 1–3 denoting incident modulus of degree of spectral coherence, and numbers 4–6 referring to scattered modulus of degree of spectral coherence.

Figures 8 and 9 show the three-dimensional (3D) moduli of the degree of spectral coherence distribution and the corresponding cross line ($\varphi = 0$) of a scattered partially polarized spatially and spectrally partially coherent EGSMP beam for different values of the pulse duration T_0 and the temporal coherence length T_{cxx}. The behaviors of the degree of spectral coherence of the incident field are also depicted in Figs. 8(d) and 9(d). As shown in Fig. 8, the value of $|\mu(rs, \omega_1, \omega_2)|$ increases as T_0 decreases. At the same time, it can be clearly found from Fig. 9 that the value of $|\mu(rs, \omega_1, \omega_2)|$ deceases with T_{cxx} rising. Furthermore, the spatial distribution remains invariant as both T_0 and T_{cxx} vary. Comparing with the incident field, the value of the degree of spectral coherence of the scattered field varies periodically with position, and the value is always less than the initial value.

4. Conclusions

In this work, based on the weak scattering theory of the first-order Born approximation, we explore the statistical properties of a scattered partially polarized spatially and spectrally partially coherent EGSMP beam irradiating on a deterministic medium. The effects of the scattering angle θ, source parameters (*i.e.*, the pulse duration T_0 and the temporal coherence length T_{cxx}), and the scatterer parameter (*i.e.*, the effective width of the medium σ_R) on the spectral density, the spectral shift, the spectral DOP and the degree of spectral coherence in the far-zero scattered field are studied numerically and comparatively. It is clearly seen that the scatter parameter barely affects the behaviors of both the spectral DOP and the degree of spectral coherence of the scattered beam, while the spectral intensity and the spectral shift rely not only on the source parameters, but also on the scatter parameter and the scattering angle. Comparing with the incident field, the values of both the spectral DOP and the degree of spectral coherence of the scattered field vary periodically with position. In addition, it is noteworthy that the effective width of the medium plays a dominant role in the spectral intensity and the spectral shift of the far-zero scattered field. Therefore, we can acquire the effective information about the scattered medium by measuring the spectral intensity and the spectral shift of a scattered partially polarized spatially and spectrally partially coherent EGSMP beam in the far-zero field.

References

[1] Wang T and Zhao D M 2010 *Opt. Lett.* **35** 2412
[2] Ding C L, Cai Y J, Zhang Y T and Pan L Z 2012 *J. Opt. Soc. Am. A* **29** 1078
[3] Ding C L, Cai Y J, Zhang Y T and Pan L Z 2012 *Phys. Lett. A* **376** 2697
[4] Du X Y 2013 *Opt. Express* **21** 22610
[5] Zhou J Y and Zhao D M 2017 *Opt. Express* **25** 17114
[6] Tsang L, Kong J A and Ding K H 2000 *Scattering of Electromagnetic Waves: Theories and Applications* (Chichester: John Wiley & Sons, Inc.) p. xi
[7] Wang X, Liu Z R and Huang K L 2017 *J. Opt. Soc. Am. B* **34** 1755
[8] Zhang Y Y and Zhou J Y 2018 *J. Opt. Soc. Am. B* **35** 2711
[9] Li J and Shi Y C 2017 *Opt. Express* **25** 22191
[10] Zhang Y Y and Zhao D M 2013 *Opt. Express* **21** 24781
[11] Wang T and Zhao D M 2010 *Chin. Phys. B* **19** 084201
[12] Liu Z R, Huang K L and Wang X 2019 *J. Opt. Soc. Am. B* **36** 3607
[13] Tong Z S and Korotkova O 2010 *Phys. Rev. A* **82** 033836
[14] Du X Y and Zhao D M 2011 *Opt. Lett.* **36** 4749
[15] Wang X, Liu Z R, Huang K L and Zhu D M 2016 *J. Opt. Soc. Am. A* **33** 1955
[16] Li J and Chang L P 2015 *Opt. Express* **23** 16602
[17] Li J, Wu P H, Chang L P and Wu Z F 2015 *Laser Phys.* **25** 096001
[18] Wang H X, Ding C L, Ma B H, Zhao C H and Pan L Z 2015 *Opt. Quantum Electron.* **47** 3365
[19] Wang H X, Ding C L, Ma B H, Zhao C H and Pan L Z 2016 *Opt. Quantum Electron.* **48** 335
[20] Lajunen H, Vahimaa P and Tervo J 2005 *J. Opt. Soc. Am. A* **22** 1536
[21] Gao M, Li Y, Lv H and Gong L 2014 *Infrared Phys. Technol.* **67** 98
[22] Li Y and Gao M 2019 *Opt. Eng.* **58** 116107
[23] Li Y and Gao M 2020 *Appl. Phys. B* **126** 34
[24] Voipio T, Setala T and Friberg A T 2013 *J. Opt. Soc. Am. A* **30** 2433
[25] Wang T, Ding Y, Ji X L and Zhao D M 2015 *J. Opt. Soc. Am. A* **32** 267
[26] Lahiri M and Wolf E 2009 *J. Opt. Soc. Am. A* **26** 2043
[27] Lajunen H, Tervo J and Vahimaa P 2004 *J. Opt. Soc. Am. A* **21** 2117
[28] Voipio T, Setala T and Friberg A T 2012 *J. Opt. Soc. Am. A* **30** 71